

A Collapsible and Motorizable Endoscopic Spiral Attachment for Safe and Efficient Intestinal Access

Alexandra Lee
Department of Mechanical Engineering
MIT
Cambridge, MA
alexlee@mit.edu

Alaz Cig
Department of Mechanical Engineering
MIT
Cambridge, MA
alaz@mit.edu

Casey Fienberg
Department of Mechanical Engineering
MIT
Cambridge, MA
caseyf@mit.edu

Max Tan
Department of Electrical Engineering and Computer MIT
Cambridge, MA
maxt114@mit.edu

Avani Narula
Department of Mechanical Engineering
MIT
Cambridge, MA
avnarula@mit.edu

Haani Mahmood
Department of Electrical Engineering and Computer Science
MIT
Cambridge, MA
haani@mit.edu

Alayo Oloko
Department of Mechanical Engineering
MIT
Cambridge, MA
alayo@mit.edu

Irma Ceco
Department of Mechanical Engineering
MIT
Cambridge, MA
iceco@mit.edu

Elena Kalodner-Martin
Comparative Media Studies
MIT
Cambridge, MA
kalodner@mit.edu

Daniel Stein
Division of Gastroenterology, Hepatology and Endoscopy
Brigham and Women's Hospital,
Harvard Medical School
Boston, MA
djstein@bwh.harvard.edu

Giovanni Traverso
Department of Mechanical Engineering
MIT
Brigham and Women's Hospital
Cambridge, MA
cgt20@mit.edu

Abstract—*Device-assisted enteroscopy is an essential procedure to evaluate and treat many conditions in the gastrointestinal tract. Current enteroscopy devices that access the ileum and jejunum are either slow and difficult or provide unfavorable risk profiles. Here, a collapsible and motorizable endoscopic spiral (CMES) attachment and proof of concept of a procedure is presented. The device uses a soft pneumatic spiral mechanism that attaches to commercial enteroscopes. The spiral can be inflated to engage with the intestine, spun to move through the tract by pleating tissue, and collapsed on demand mid-procedure to be withdrawn in case of complication. We evaluate movement rate by pleating in ex vivo swine models, characterize the inflation-deflation properties of the spiral, and validate articulation combined with commercial endoscopes. By improving procedure ease, efficiency, and safety, CMES can improve access to gastrointestinal care and resolve unmet clinical needs.*

Keywords—*Medical devices, endoscopy, soft robotics, biomedical engineering, gastroenterology*

I. INTRODUCTION

A. Motivation: Accessing the small intestine

Effective treatment of many gastrointestinal (GI) conditions requires accessing, imaging, and intervening along the complete

length of the small intestine (SI) [1]. There are 3.8 million hospital admissions annually in the U.S. for GI related diagnoses, costing around \$110 billion in annual health care expenditures [2]. Delayed diagnosis in obscure GI bleeding alone can result in a 13% increase in mortality [3]. To diagnose and treat these GI conditions, endoscopic evaluation of the GI tract is an essential procedure for direct examination and interaction with GI organs. When direct access isn't required, non-invasive imaging methods including capsule endoscopy, magnetic resonance imaging, and computed tomography are available for diagnostic evaluation. However, enteroscopy provides direct access inside the body for clinicians to visually evaluate the SI in real-time, explore specific sites, collect targeted biopsies, and perform concurrent therapeutic procedures such as polypectomy or hemostasis [4,5].

The SI has three segments: duodenum, jejunum, and ileum. The SI past the early jejunum is referred to as the deep SI in this paper. The SI is primarily composed of soft and viscoelastic tissue with both inter-patient and location-specific dimensional and mechanical variations. Human intestinal tissue is heterogenous and has anisotropic properties with an average elastic modulus of 2.63 MPa [6]. The inner diameter of the jejunum is on average 30 mm and the inner diameter of the ileum is 20-25 mm; the SI length can be 3-5 m [7].

The push enteroscopy procedure, while common, is not capable of accessing the SI past the early jejunum. Push enteroscopy entails manually pushing a scope to advance

through the GI tract. Advancing by push enteroscopy fails in the deep SI due to insufficient anchoring and scope buckling [8]; the scope cannot advance further beyond 5-10% of the entire SI length. Past the early jejunum, the mesentery anchoring the SI is reduced. Additionally, due to the increased tortuosity of the tract and low stiffness of the scope, the scope starts to buckle and loop with further pushing. More advanced procedures and systems have been developed with the goal of accessing the deep SI [1].

B. Current small intestine access methods

Current devices for accessing the deep SI are either slow and difficult or provide unfavorable risk profiles. These systems build on push enteroscopy by using balloons to sequentially anchor, soft robotics with pneumatic actuation, or spirals to pleat the intestine. While these systems can reach the SI, the current clinically available methods are slow and difficult while other methods have high complexity or poor risk profiles.

Double-balloon enteroscopy (DBE) is the first choice method for direct, deep SI access. DBE uses two balloons on an overtube with a manual push-and-pull technique to sequentially inflate, anchor to the SI, and move. Due to the repetitive and manual process, DBE requires extensive clinical training, high capital expenditure, specialized equipment, and is slow, consuming one to three hours per procedure. Single balloon enteroscopy uses one balloon to simplify the procedure, slightly reducing training and equipment needs but still with similar limitations. Compared to DBE, single balloon enteroscopy is less successful traversing deep into the SI [8].

Research-grade soft robotic systems, such as vine-like and inchworm-like mechanisms, use pneumatics to morph and traverse through the GI tract [9,10]. These devices are not approved by regulatory agencies and are likely to face translational challenges due to cost, risk, usage difficulty, and mechanical complexity.

The now defunct spiral enteroscopy (SE) method uses an overtube with a spiral at the distal end to access the SI by pleating [11]. SE was introduced to the US in 2008 by Spirus Medical. The clinician spins the spiral and the spiral's threads engage with the luminal tissue of the intestine, pleating the intestine over the scope and moving the scope forward through the GI tract faster than balloon-based methods [11,12]. Manual SE was laborious and the device required two people to operate [13]. A motorized version was developed, boasting an average procedure time of 60 minutes [11]. However, adverse complications occurred during motorized SE, including esophageal lacerations and mechanical failure mid-procedure. The motorized SE device was recalled following a patient death [11].

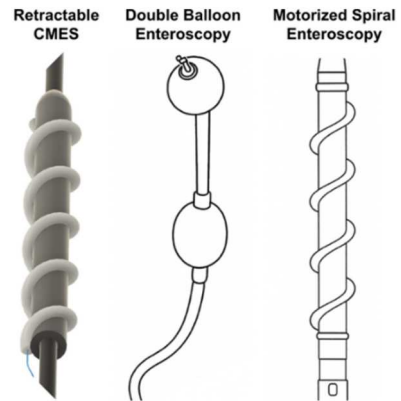


Fig. 1. Comparison of endoscopic deep SI access devices.

C. A collapsible and motorizable endoscopic spiral

CMES addresses the unmet clinical need of easier, safer, and more accessible SI evaluation and intervention. Inspired by the efficiency of motorized SE and the safety profile of DBE, we developed a collapsible and motorizable endoscopic spiral (CMES) attachment (Fig. 1). A soft collapsible pneumatic spiral mechanism was designed to traverse the SI like established rigid SE systems, plus engage and disengage on demand while in the body. This collapsible mechanism allows for safe and quick removal in the event of a complication and potentially safer passage through the esophagus. CMES is designed as a low-cost universal attachment compatible with different commercially available endoscopes. Thus, CMES provides improved speed, ease, and risk profiles compared to state-of-the-art intestinal access methods. Collectively, these results establish CMES as an SI evaluation and intervention method with clinical efficiency and translational practicality.

D. Mechanics of spiral pleating

The mechanics of enteric spiral pleating can be modeled using the principles of screws [14]. As a screw rotates, the threads engage with the surrounding to advance or retract material. Thread-to-material engagement is dependent on factors such as contact area, thread geometry (including height, pitch, and inner/outer diameter), and the normal force the threads exert (Fig. 2). In SE, these screw-driven material displacement mechanics are utilized to navigate the SI: when inserted and rotated, the spiral engages with the intestine's luminal tissue and pulls the tissue over the scope, pleating folds of tissue. This allows the scope to advance and retract through the SI. The viscoelastic and heterogeneous tissue pleating with the spiral in the complex abdominal cavity constitutes a challenging mechanics problem.

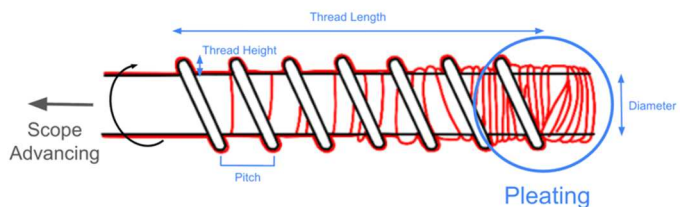


Fig. 2. Spiral pleating mechanics and key parameters.

II. METHODS

The following key functional requirements for the system were identified: dimensional compatibility to pass through the esophagus and fit inside the intestine while fitting over the endoscope; biocompatibility with the GI tract; engagement with the intestine's luminal tissue for effective pleating; mechanical robustness when pressing against the intestine; fast advancement in the GI tract; articulation around anatomical curves, and quick disengagement. A core mechanical challenge is to achieve sufficient stiffness to engage the intestine while being able to morph and disengage easily with on-demand changes in mechanical stress.

A. Design and fabrication

Two design strategies were explored: a thermoformed spiral and a pneumatic thread spiral. Both were created from a 12 mm thick 80A thermoplastic polyurethane (TPU) sheet and heat sealed via a 12 inch impulse sealer. The key difference between the configurations is that the thermoformed spiral has jointly inflated threads and core while the pneumatic thread spiral has only pneumatically inflated threads.

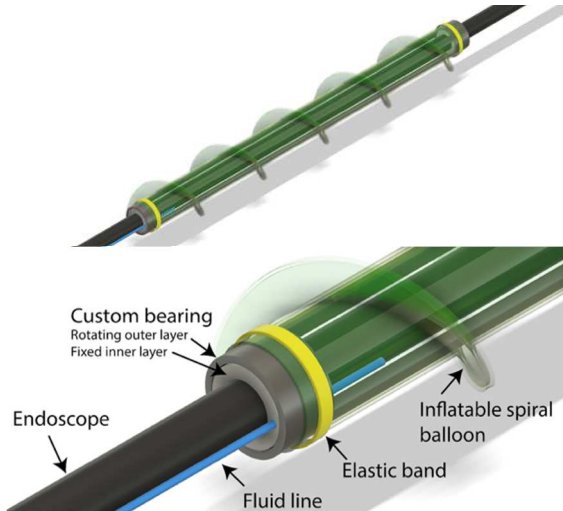


Fig. 3. Model of thermoformed system. System assembled on the endoscope (top). Close-up of the design's components (bottom). The motor interface is not displayed.

The thermoformed spiral stiffens and collapses with the inflation and deflation of both the core and threads (Fig. 3, 4). It consists of a double layered cylindrical TPU sleeve with joined TPU threads protruding from the outer surface. When the device is pressurized, air enters from the inner cavity between layers and stiffens the sleeve. A mold of a flattened spiral was 3D printed (Prusa MK4) and used to thermoform discontinuous spirals from a sheet of TPU via a vacuum former (Formech 450DT). The spiral and its base form the outer layer; the outer layer is heat-sealed to a second sheet of TPU forming the inner layer. Holes were created on the inner layer beneath the spiral with a soldering iron for air to reach and inflate the threads. Finally, the longitudinal edges of the piece were heat-sealed together to create a tubular shape. At 3 psi, the thermoformed spiral mimics the dimensions of the Olympus PowerSpiral with

a pitch of 48 mm and inner diameter of 18.1 mm; the entire sleeve is 30 cm long.



Fig. 4. Physical prototype of the inflated thermoformed system.

The pneumatic thread strategy features a continuous inflatable thread attached to a flexible overtube (Fig. 5, 6). To create the threads, a TPU sheet was folded in half and heat-sealed in three places: one seal parallel to the fold, and two seals perpendicular to the fold. The helical balloon was adhered to the flexible overtube with 3M Scotch-Weld plastic glue. The inner diameter of the overtube is 14 mm, outer diameter is 18 mm, and the spiral thread pitch is 29 mm, mimicking the Spirus, with a total thread length of 140 mm.



Fig. 5. Model of the pneumatic thread system. The white thread is the only inflatable portion.



Fig. 6. Physical prototype of the inflated pneumatic thread system.

B. Experimental methods

Experiments were conducted to evaluate the ability to traverse by pleating, to characterize the inflation-deflation properties of the spiral, and to validate the compatibility of the design's mechanical properties with commercial endoscopes.

1) Ex vivo pleating evaluation

To evaluate pleating ability, ex vivo swine intestinal tissue specifically from the jejunum and ileum was used as a model. The intestine was excised from a freshly harvested GI tract and rinsed. Meter long segments were cut and stored at -80°C. Each segment was thawed for 24 hours at 4°C before data collection to minimize degradation and assure consistency. A custom test rig was constructed to suspend the intestine, mimicking the mechanical constraints and suspension of the deep SI in the abdominal cavity (Fig. 7). The rig was built from two vertical PVC supports with a horizontal PVC beam between. Slidable clips allowed the intestine to be suspended by its membrane.

This setup provided minimal rigid support while suspending the sample, allowing the tissue to bunch and shift freely, simulating the in vivo environment of the SI.

During testing, the opening of the intestine section was fixed in place where spiral prototypes were inserted. Once each prototype was fully inserted, the device was manually rotated with the device shaft fixed in position. To maintain tissue hydration and to replicate in vivo lubrication conditions, the intestine was periodically sprayed with phosphate buffered saline. Experiments were done within two-hour intervals to avoid the effects of tissue degradation. Initial testing with preliminary prototypes compared diameters, pitches, and materials to establish a range for parameters. Quantitative measurements were collected on prototypes with the pneumatic thread design.

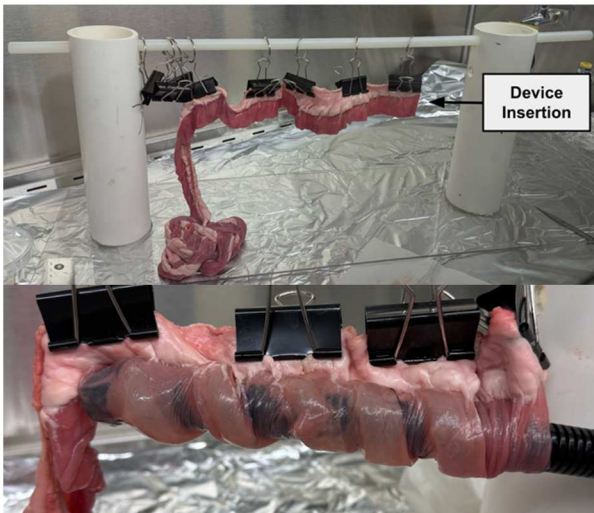


Fig. 7. Ex vivo characterization of pleating with swine SI. In the setup (top), the intestine is suspended by membrane to replicate the in vivo environment. The device engages the suspended SI to pleat and move (bottom).

To quantify pleating, a reference point was first set on the intestine's outer surface with a surgical ink fiducial marker. The distance was measured by ruler from the distal tip of the device to the fiducial marker, at every set of turns n . The distance the device advanced was calculated (Eq. 1, 2). Nonzero distance advanced was considered successful pleating for initial ex vivo.

$$\text{Distance}(n) = \text{Position}_{\text{Distal tip}}(n) - \text{Position}_{\text{Fiducial}}(n) \quad (1)$$

$$\text{Distance advanced}(n) = \text{Distance}(n) - \text{Distance}(0) \quad (2)$$

2) Inflation-deflation characterization

The outer diameter of the spiral is critical for safe passage, removal, and spiral engagement. The dimensional response, measured by outer diameter of the spiral, to pressure change was characterized using a pump with an integrated pressure gauge (eBall). A caliper was used to measure the spiral outer diameter at different internal pressures.

3) Validating articulation compatibility with endoscope

To successfully navigate anatomical curves, the flexible spiral must not affect the articulation of the endoscope. The bending stiffness and the minimum bending radius are critical

metrics to compare between the endoscope with and without CMES. Together, the metrics represent force required to turn and sharpest turn possible. A dual channel Pentax EG-3890TK was used as an example of a commercially available endoscope. Qualitatively, a camera and fixed tripod were used to record the cantilever bending of the endoscope due to gravity with and without CMES to visualize impact of the device on the endoscope's articulation.

III. RESULTS

A. CMES can match the pleating efficiency of rigid motorizable spirals in ex vivo swine model

Initial testing with prototypes compared diameters, pitches, and materials to establish a range for effective intestinal pleating. Table 1 shows how various geometry and material combinations affect pleating ex vivo. The pneumatic thread spiral design performed more regular pleating than the thermoformed spiral, so the pneumatic thread spiral was used for further investigation.

TABLE I. SPIRAL GEOMETRY AND EFFECTS ON EX VIVO PLEATING

Material (Core – Shaft)	Inner-Outer Diameter (mm)	Pitch (mm)	Engages Tissue	Rotates in Intestine	Pleating (Engage \cap Rotate)	Collapse On Demand
PVC-Wood	5-10	46	X	✓	X	X
Glue-PVC	13-27	53	X	✓	X	X
Glue-PVC	25-39	57	✓	X	X	X
Glue-PVC	19-35	52	✓	✓	✓	X
TPU-PVC	19-36	58	✓	✓	✓	✓
TPU-TPU	28-31	43	✓	X	X	✓
Spirus (+)	17-29	29	✓	✓	✓	X

The ex vivo advancement by pleating experiment shows the pneumatic thread spiral was able to effectively engage the intestine's luminal tissue and pleat at a rate comparable to or better than positive control, the rigid Spirus (Fig. 8). The device performed slightly worse than a fully rigid solid spiral of the same dimensions. This comparable rate was generally sustained over the measured 10 spiral turns reaching 12.97 ± 0.34 cm (n=3, mean \pm SD).

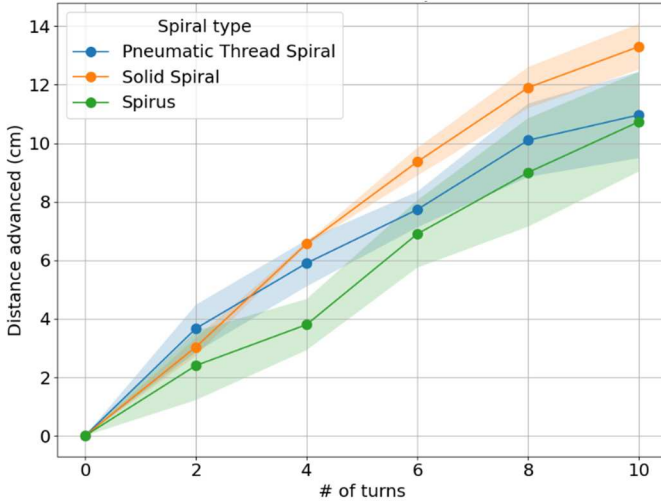


Fig. 8. Distance advanced by pleating over number of turns (n=3, ± 1 SD shaded).

B. CMES can inflate to beyond lumen size of intestine and deflate to below lumen size of intestine on demand

When inflated CMES can reach sizes engaging with the intestine and when deflated CMES can shrink to sizes smaller than the intestine (Fig. 9). When pressurized, the CMES outer diameter reaches sizes comparable to the positive control rigid spiral. Upon depressurization, CMES shrinks and rapidly disengages the intestine – a safety feature the Spirus and Olympus devices lack.

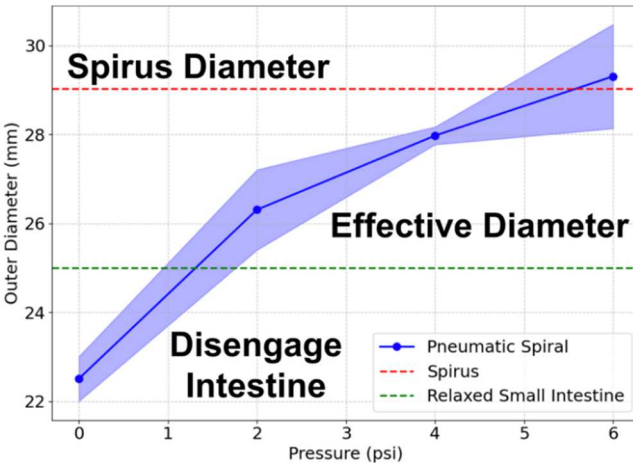


Fig. 9. Outer diameter of CMES pneumatic spiral over varied pressures (n=3, ± 1 SD shaded).

C. CMES does not majorly curtail the articulation of a commercial endoscope

Based on qualitative comparisons of the endoscope with and without CMES, there are no major changes in cantilever bending and minimum bending radius. These metrics are critical to the articulation and navigation of the endoscope *in vivo*. The endoscope alone is used as positive control.

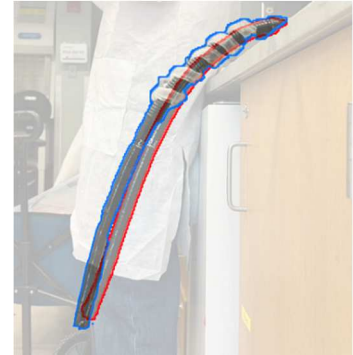


Fig. 10. Comparison of cantilever bending between endoscope with and without CMES. The red outline shows bending of standalone endoscope (positive control); the blue outline shows bending of endoscope with CMES.

The observed difference in cantilever bending deflection is minimal (Fig. 10). This implies that the addition of the inflatable spiral does not significantly change the flexibility of the endoscope. This was confirmed during the bending radius test where the scope was bent with and without the CMES spiral to the minimum possible radius, showing no major restriction (Fig. 11).



Fig. 11. Comparison of minimum bending radius between endoscope with CMES (left) and without CMES (right, positive control).

IV. CONCLUSION

CMES uses a pneumatic soft spiral mechanism to enable safe and efficient endoscopic intestinal access. We demonstrate that CMES can traverse the SI by pleating and collapsing on demand. Compared to DBE, CMES enables a streamlined procedure to access the deep SI more easily and quickly with less equipment. Compared to SE, CMES provides a safer risk profile due to the device's collapsibility and softness. While other soft robotic device-assisted enteroscopy methods have not reached the clinic at scale, CMES is expected to close the translational gap thanks to the design's ease of use.

Future work will focus on the development of a complete enteroscopy platform. CMES is designed to be attached via bearings with pneumatic tubing along the endoscope. While the rotating and pneumatic components of the device can be connected by a rotary union, it could prove difficult due to size constraints. Inflation control can be developed with real-time closed-loop pressure control and smoother integration with existing enteroscopy workflows. Ex vivo characterization is required to evaluate the effects of motor torque and speed on tissue health and advancement speed. In vivo testing of safety and effectiveness in large animals, accounting for various complications and emergencies, would prepare CMES for clinical translation. Future soft robotic endoscopy devices focused on mechanical simplicity and integration with clinical workflows can improve access to GI care.

REFERENCES

[1] Schneider, M., Höllerich, J., and Beyna, T., 2019, “Device-Assisted Enteroscopy: A Review of Available Techniques and Upcoming New Technologies,” *World J Gastroenterol*, 25(27), pp. 3538–3545. <https://doi.org/10.3748/wjg.v25.i27.3538>.

[2] Peery, A. F., Murphy, C. C., Anderson, C., Jensen, E. T., Deutsch-Link, S., Egberg, M. D., Lund, J. L., Subramaniam, D., Dellon, E. S., Sperber, A. D., Palsson, O. S., Pate, V., Baron, T. H., Moon, A. M., Shaheen, N. J., and Sandler, R. S., 2025, “Burden and Cost of Gastrointestinal, Liver, and Pancreatic Diseases in the United States: Update 2024,” *Gastroenterology*, 168(5), pp. 1000–1024. <https://doi.org/10.1053/j.gastro.2024.12.029>.

[3] Raju, G. S., Gerson, L., Das, A., and Lewis, B., 2007, “American Gastroenterological Association (AGA) Institute Technical Review on Obscure Gastrointestinal Bleeding,” *Gastroenterology*, 133(5), pp. 1697–1717. <https://doi.org/10.1053/j.gastro.2007.06.007>.

[4] Yamamoto, H., Yano, T., Kita, H., Sunada, K., Ido, K., and Sugano, K., 2003, “New System of Double-Balloon Enteroscopy for Diagnosis and Treatment of Small Intestinal Disorders,” *Gastroenterology*, 125(5), pp. 1556; author reply 1556–1557. <https://doi.org/10.1016/j.gastro.2003.03.004>.

[5] Lewis, B. S., 1999, “The History of Enteroscopy,” *Gastrointest Endosc Clin N Am*, 9(1), pp. 1–11.

[6] Hosseini, H. S., and Dunn, J. C. Y., 2020, “Biomechanical Force Prediction for Lengthening of Small Intestine during Distraction Enterogenesis,” *Bioengineering (Basel)*, 7(4), p. 140. <https://doi.org/10.3390/bioengineering7040140>.

[7] Nam, H. G., and Miftahof, R. N., eds., 2010, “Biomechanics of the Small Intestine,” *Mathematical Foundations and Biomechanics of the Digestive System*, Cambridge University Press, Cambridge, pp. 157–181. <https://doi.org/10.1017/CBO9780511711961.011>.

[8] Singeap, A.-M., Sfarti, C., Minea, H., Chiriac, S., Cuciureanu, T., Nastasa, R., Stanciu, C., and Trifan, A., 2023, “Small Bowel Capsule Endoscopy and Enteroscopy: A Shoulder-to-Shoulder Race,” *J Clin Med*, 12(23), p. 7328. <https://doi.org/10.3390/jcm12237328>.

[9] Pore, A., Piccinelli, N., Rossi, G. D., Piano, M., Meli, D., Dall’Alba, D., Muradore, R., and Fiorini, P., “EndoVine: Soft Robotic Endoscope for Colonoscopy.”

[10] Bernth, J. E., Zhang, G., Malas, D., Abrahams, G., Hayee, B., and Liu, H., 2024, “MorphGI: A Self-Propelling Soft Robotic Endoscope Through Morphing Shape,” *Soft Robotics*, 11(4), pp. 670–683. <https://doi.org/10.1089/soro.2023.0096>.

[11] Xiao, S.-P., Lin, H., and Chen, H.-B., 2024, “Motorized Spiral Enteroscopy: A Cautious Step Forward in Technological Innovation,” *World J Gastrointest Endosc*, 16(11), pp. 581–586. <https://doi.org/10.4253/wjge.v16.i11.581>.

[12] Akerman, P. A., Agrawal, D., Cantero, D., and Pangtay, J., 2008, “Spiral Enteroscopy with the New DSB Overtube: A Novel Technique for Deep Peroral Small-Bowel Intubation,” *Endoscopy*, 40, pp. 974–978. <https://doi.org/10.1055/s-0028-1103402>.

[13] Mussetto, A., Merola, E., Casadei, C., Salvi, D., Fornaroli, F., Cocca, S., Trebbi, M., Gabbielli, A., Spada, C., and Michielan, A., 2024, “Device-Assisted Enteroscopy: Are We Ready to Dismiss the Spiral?,” *World J Gastroenterol*, 30(26), pp. 3185–3192. <https://doi.org/10.3748/wjg.v30.i26.3185>.